Journal of Peptide Science
J. Peptide Sci. **11**: 536–545 (2005)
Published online 3 May 2005 in Wiley InterScience (www.interscience.wiley.com). DOI: 10.1002/psc.672

JOURNAL OF PEPTIDE SCIENCE

Circular dichroism spectroscopic study of non-covalent interactions of poly-L-glutamic acid with a porphyrin derivative in aqueous solutions

LUKÁŠ PALIVEC,[a] MARIE URBANOVÁ[b]* and KAREL VOLKA[a]

[a] Department of Analytical Chemistry, Institute of Chemical Technology, Technická 5, 166 28 Praha 6, Czech Republic
[b] Department of Physics and Measurements, Institute of Chemical Technology, Technická 5, 166 28 Praha 6, Czech Republic

Received 12 October 2004; Accepted 26 January 2005

Abstract: The interactions of poly-L-glutamic acid and a cationic porphyrin derivative in aqueous solutions were studied by the combination of vibrational circular dichroism (VCD) and electronic circular dichroism (ECD) spectroscopies. It was found that non-covalent interactions between both agents influence the structure of the polymeric matrix and the guest porphyrins and *vice versa*, but the physico-chemical properties of the solutions, especially the pH and the relative permittivity of the solvent, play a key role in the structure of the polypeptide part of the formed complexes. It was shown that the interaction with porphyrins prevents the precipitation of poly-L-glutamic acid in aqueous solution at acidic pH. In special conditions, the porphyrins attached to the polypeptide probably possess face-to-face interaction as demonstrated by the enhancement of the characteristic ECD signal and the appearance of sidebands on its short and long wavelength sides. Copyright © 2005 European Peptide Society and John Wiley & Sons, Ltd.

Keywords: vibrational circular dichroism; electronic circular dichroism; poly-L-glutamic acid; porphyrin; interaction; structure

INTRODUCTION

During the past few decades it has been discovered that porphyrins are effective photosensitizers with potential use in the photodynamic therapy of cancer. It was proved that the required selective destruction of tumour tissue by a polypeptide–porphyrin conjugate was more effective compared with a non-conjugated porphyrin [1]. The properties of polypeptide–porphyrin conjugates are significantly affected by the spatial arrangement of the polypeptide matrixes whose secondary structure was closely investigated and described [2]. Spectroscopic techniques, namely FTIR absorption [3,4] and NMR spectroscopy [5–7], proved suitable for the study of the polypeptide secondary structure. Due to the fact that a polypeptide chain shows optical activity, dichroic spectroscopic methods including optical rotatory dispersion [8], electronic circular dichroism (ECD) [9], Raman optical activity [10–13] and vibrational circular dichroism (VCD) [12,14–21] were also used. Of these, VCD, which is the vibrational analogue of the more widespread ECD, showed high sensitivity to the polypeptide structure. This fact, along with development and progress in computational *ab initio* techniques [22–25] which have been applied to oligopeptides [26–29], make VCD an efficient tool for the conformational study of peptides.

It is well known that secondary structure, which depends on intramolecular hydrogen bonds, is influenced by the physicochemical properties of solution [30] and polypeptide conformational changes have been described [14,31–34]. Therefore, polypeptides can serve as polymeric spatially aligned matrices, which are able to imprint their geometric properties onto the interacting porphyrins [35–40]. A large induced ECD signal in the Soret region, which is characteristic for porphyrins, was observed in non-covalent complexes [37–39] as well as in covalent porphyrin–peptide conjugates [35]. The induction of porphyrin optical activity is not caused only by large macromolecules such as polypeptides but also by small chiral molecules, for example amino acids [41]. As another example, originally achiral porphyrin tweezers and bis-porphyrins exhibit exciton coupled CD curves after complexation with chiral amines and other chiral guests [42–45]. The positions of two porphyrin molecules were defined in the different bis-porphyrin derivatives of steroidal diols. In such systems, the porphyrin coupling was manifested in the ECD spectra and was studied in detail experimentally and using computational methods [46].

The ionic interaction between homopolypeptides and porphyrins has already been studied in systems composed of cationic poly-L-lysine and anionic *meso*-tetrakis(4-sulfonatophenyl)porphyrin (TPPS). The porphyrin part of the complexes was characterized [37–39] and the structure of the oligopeptide part of the complexes was discussed [47]. Cationic porphyrins are also widely studied because of their binding to the biologically important polymer DNA [48] in which the cleavage

*Correspondence to: M. Urbanová, Department of Physics and Measurements, Institute of Chemical Technology, Technická 5, 166 28 Praha 6, Czech Republic; e-mail: marie.urbanova@vscht.cz

of nucleic acids can be caused by energy transfer through the porphyrin triplet states via production of singlet oxygen. The understanding of the interaction of a cationic porphyrin to another *in vivo* abundant polymeric structure, protein, is a further challenging task. One such model system of proteins which is endowed with the ability of ionic interaction with cationic porphyrins is polyglutamic acid [37,39,49]. As far as is known, possible variations in the secondary structure of this polypeptide matrix caused by non-covalent interaction with porphyrins has not been notified yet.

The secondary structure of poly-L-glutamic acid (PLGA) can be tuned by physico-chemical conditions. In aqueous solution at neutral and basic pH, it is composed of restricted structural elements which were shown to be conformationally similar to the left handed 3_1 polyproline II helix [9,50,51]. For simplicity, this secondary structure is indicated as PPII in this paper. At acidic pH in concentrations of ~0.01 mol/l which are suitable for ECD measurements, the α-helix conformation of PLGA was detected on the basis of a characteristic ECD signal [37–39,52]. At concentrations more than 10 times higher than are necessary for IR spectral study, no observations of α-helix PLGA conformation in aqueous solutions at acidic pH have been published. A dioxan/H_2O mixture at acidic pH was found to be a solvent suitable for the formation of the α-helix conformation in PLGA concentrated solution [8]. In addition, the presence of dioxan prevents the precipitation of PLGA, probably owing to solvation of the side chain COOH groups. However, dioxan also prevents the interaction between polypeptide and porphyrin. In general, alcohols are other solvents that support α-helix formation [53]. Due to these facts, new conditions suitable for the study of interaction with α-helix PLGA need to be tested and its characterization is one of the goals of this paper.

In this paper, systems composed of *meso*-tetrakis (α-trimethylammonio-*p*-tolyl)porphyrin tetrabromide (TATP) and PLGA were studied. TATP was chosen as an appropriate cationic porphyrin derivative with great solubility in polar solvents and very weak undesirable self-aggregation [48,54]. PLGA is not only an appropriate counterpartner for ionic interaction with cationic TATP due to its COOH side groups, but is also suitable for testing the influence of the matrix secondary structure on the polypeptide–porphyrin interaction. VCD spectroscopy was employed in the structural study of the polypeptide part of the complexes. This methodology not only monitors the secondary structure of polypeptides and proteins very sensitively, but also detects short-range structural variations [20], and is therefore able to register very subtle changes in structure caused by non-covalent interactions. Absorption and circular dichroism spectroscopy in the UV-VIS region were used for the characterization of the porphyrin part of the complexes. The ECD technique is suitable for observation of the imprinted spatial arrangement of the porphyrin derivatives as well as for the estimation of the polypeptide secondary structure at lower concentrations. Although the induction of the porphyrin optical activity due to interaction with polypeptides was reported previously [37–39], the conformational changes of polypeptides after binding of porphyrins, as well as the characterization of porphyrin association during the polypeptide–porphyrin complexation, were not described thoroughly and were neglected in studies dealing with polypeptide–porphyrin interactions. In this paper, a combination of circular dichroic and absorption techniques in both the UV-vis and IR regions was shown to be a powerful tool for the study of macromolecular chiral assemblies.

MATERIALS AND METHODS

The sodium salt of poly-L-glutamic acid with average molecular weights of 50 300, 17 000, 10 900 ($PLGA_{50,300}$, $PLGA_{17,000}$, $PLGA_{10,900}$) and *meso*-tetrakis(4-sulfonatophenyl)porphyrin tetra sodium salt (TPPS), purity higher than 98%, were purchased from Sigma Aldrich. *Meso*-tetrakis(α-trimethylammonio-*p*-tolyl)porphyrin tetrabromide (TATP, Scheme 1) of a purity higher than 98% was prepared in the Department of Analytical Chemistry, Institute of Chemical Technology, Prague, and characterized previously [48]. All reagents were used without further purification. The deuterated solvents D_2O (≥99.9% atom D) and methanol-d_4 (≥99.8% atom D) were purchased from Isosar GmbH, and 1,4-dioxan-d_8 (≥99% atom D) was purchased from Merck. 11% DCl/D_2O (v/v) and 20% NaOD/D_2O (w/w) solvents were used for pH adjustment.

For the VCD measurements, PLGA as well as TATP were dissolved in deuterated solvent and an appropriate volume of TATP stock solution was added to the PLGA solution. The concentration of PLGA was chosen so that the absorbance in the region 1800–1350 cm^{-1} was between 0.2 and 0.8 in the 25 μm pathlength cell and is given on a polypeptide residue. Its value was kept at 0.39 mol/l, whereas the porphyrin concentration depended on the desired ratio $R = [P]/[D]$, where $[P]$ is the glutamic acid residue concentration and $[D]$ is the concentration of the porphyrin derivative. For UV-VIS and ECD measurements double distilled water was used.

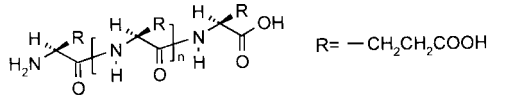

poly-L-glutamic acid

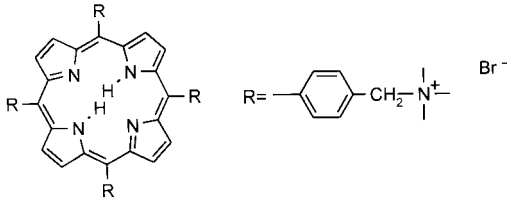

meso-tetrakis(α-trimethylammonio-*p*-tolyl)porphyrin tetrabromide

Scheme 1

The concentration of the porphyrin derivative was kept at 5×10^{-6} mol/l for UV absorption and 2.5×10^{-5} mol/l for ECD, respectively, the concentration of PLGA was given by the desired value of *R*. The pH of the solutions was measured on a Cole Parmer pH meter with a glass microelectrode (9802BN Orion) before each spectral measurement. In this paper, the pH was measured not only in pure H_2O (D_2O) solutions, but also in the presence of methanol and dioxan. No correction of the measured pH was done, so the pH is given as approximate values (pH ~ 5, pH ~ 8).

The VCD and infrared absorption spectra were measured in the 1800–1350 cm^{-1} region at room temperature with a resolution of 8 cm^{-1} on a FTIR IFS 66/S spectrometer equipped with a VCD/IRRAS module PMA 37 (Bruker, Germany) as described previously [55]. A demountable cell with CaF_2 windows and a teflon spacer of 25 μm pathlength was used. The VCD spectra were normalized to $A = 1$ for the amide I absorption band but the absorption spectra given in the figures show the actual measured values. All the VCD spectra are averages of six blocks of scans, each block counting 3680 scans (20 min), the noise spectra were calculated as the standard deviation and typical values are shown in Figure 3. The S/N of other VCD spectra is very similar and the noise spectra are not shown for simplicity in the other figures. The averaged VCD spectra were corrected for the baseline, which was obtained as the VCD spectrum of the solvent measured in the same conditions. The absorption spectra were corrected for the solvent absorption.

The UV-VIS absorption measurements were carried on a CARY 400 spectrophotometer (Varian, Australia) with a spectral resolution of 1 nm, a scan rate of 600 nm/min, and a 1 cm silica quartz cell was used. ECD measurements were performed on a CD 6 spectrophotometer (ISA Jobin Yvon-Spex, France), with a spectral resolution of 0.5 nm, an integration time of 2 s for each spectral point, using silica quartz cell of pathlength 0.2 for Soret and 0.1 cm for peptide regions, respectively.

RESULTS

Conformation of Pure PLGA at High Concentrations

Figure 1 shows the VCD spectra of PLGA in aqueous and mixed aqueous solutions in the amide I region observed at different pH values. At pH ~ 8, the negatively biased VCD couplet with a negative band centred at 1639 cm^{-1} was observed independently of the addition of methanol-d_4 or dioxan-d_8 into mixed aqueous solutions. The positive band was observed at 1664, 1666 and 1670 cm^{-1} in the D_2O, methanol-d_4/D_2O and dioxan-d_8/D_2O solutions, respectively (spectra (a)–(e)). The negative couplets were centred at 1649 cm^{-1} and correspond to the amide I absorption (Figure 1, ABS). At pH ~ 8, most of the side chain groups existed as carboxylate anions and the characteristic absorption bands at 1564 and 1403 cm^{-1} occurred assigned to asymmetric and symmetric vibrations of COO^- groups, respectively. At pH ~ 5, the precipitation of PLGA occurred in both the aqueous and methanol-d_4/D_2O solutions in

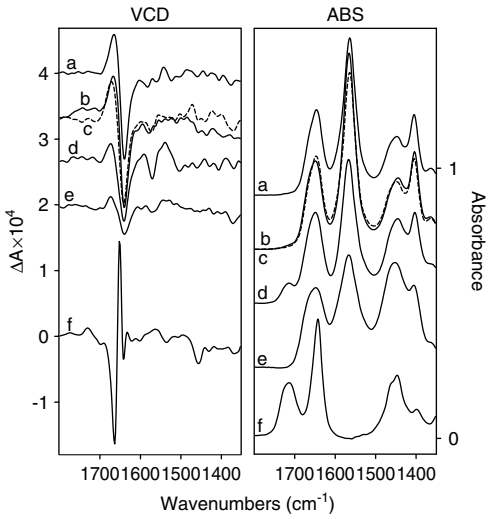

Figure 1 VCD and IR absorption spectra of PLGA at pH ~ 8 in D_2O (a), 20% methanol-d_4/D_2O (b), 40% methanol-d_4/D_2O (c), 60% methanol-d_4/D_2O (d), 50% dioxan-d_8/D_2O (e), and at pH ~ 5 in 50% dioxan-d_8/D_2O (f).

the concentration range used for IR measurements (~0.4 mol/l), while a homogeneous PLGA solution was obtained in 50% dioxan-d_8/D_2O mixed solvent. A strong positive conservative VCD couplet consisting of positive and negative bands at 1651 and 1663 cm^{-1}, respectively, of nearly the same intensity and a small negative sideband on the short wavelength side at 1640 cm^{-1} were observed in this case (Figure 1f). The distinctive spectral features observed at different pH values in the amide I region evidently arise from different chain structures. The negative VCD couplet obtained for pH ~ 8 is typical of the PPII conformation reported for different polypeptides [14,50] and was observed for PLGA previously [50]. The positive couplet obtained for the dioxan-d_8/D_2O solution at pH ~ 5 is typical of the α-helix structure [17]. Such a pronounced α-helix shape was not reported for PLGA solutions previously, however, early measurements [15] reported the PLGA spectra as a helix conformation.

The negatively biased negative VCD couplet characteristic of the PPII structure was observed for all solvents used at pH ~ 8. However, the peak intensities of the negative as well as the positive bands were different, depending on the solvents used. The negative and positive signals of PLGA in D_2O (spectrum (a)) exhibited the biggest magnitude in comparison with VCD in other solutions. The presence of 20%, and even 40% methanol-d_4 in D_2O (spectra (b), (c)) did not cause considerable changes in the VCD signal shape. However, the VCD intensity (the positive-negative peak-to-peak $\Delta A/A_{max}$ value in amide I region) was substantially reduced by the addition of 60% methanol-d_4 or 50% dioxan-d_8 into D_2O solvent (spectra (d), (e)). Accordingly, simultaneous variations in the absorption spectra changes (Figure 1, ABS) were observed. In the presence

of 60% methanol-d_4 at pH ~ 8 or 50% dioxan-d_8 in D_2O at pH ~ 5 (spectra (d), (f)), the absorption band at 1713 cm^{-1} caused by the C=O stretch vibration of the side chain COOH groups occurred simultaneously with a decrease in the band intensity corresponding to asymmetric and symmetric COO^- vibrations located at 1564 and 1403 cm^{-1}, respectively. In the mixed solvents containing more than 50% methanol-d_4 or dioxan-d_8, a decrease in the VCD band intensity characteristic for PPII structure was observed. The peak-to-peak $\Delta A/A_{max}$ value in amide I region was reduced to about one third of that measured in the D_2O solution at pH ~ 8.

At a concentration up to 0.025 mol/l of the PLGA residue, the transition of the PLGA secondary structure from PPII to α-helix caused by lowering the pH in aqueous solutions and mixed MeOH/H_2O was reported [30,53]. In the concentration used for IR absorption and VCD studies (more than 10 times higher), the precipitation of pure PLGA occurred in aqueous and methanol-d_4/D_2O solutions at pH ~ 5. In addition to the low pH, the presence of dioxan-d_8 in D_2O, 50% (v/v) at least, is necessary to obtain a nonprecipitating solution that shows the VCD signal typical of the α-helix structure.

The Interaction of PLGA with Porphyrin Derivative

The intramolecular interactions of porphyrins and the porphyrin interactions with the polypeptide matrix were followed using UV-VIS absorption. Figure 2 shows the absorption spectra in the Soret region of TATP and the PLGA-TATP, $R = 100$, dissolved in aqueous and mixed aqueous solvents. It was established that the ratio R of PLGA/TATP had no significant influence on the UV-VIS spectra in the range $R = 10–100$. A value $R = 100$ was chosen as suitable for the ECD measurement because the corresponding concentrations of TATP and PLGA are appropriate for the measurements in both Soret and peptide regions. Values of pH ~ 8 and pH ~ 5 were chosen in order to obtain two different conformations of the PLGA matrices. Simultaneously, the acidic pH value was kept higher than the dissociation constant of TATP ($pK_a = 4.7$) to minimize the protonation of the TATP porphyrin ring. Without PLGA, the absorption spectra showed a dominant Soret band typical of monomeric porphyrin in agreement with studies on self-aggregation of the *meso*-tetratolylporphyrins [48,54]. In the presence of PLGA, the absorption bands showed hypochromism and red shift (414 → 424 nm) for both pH values (Figure 2A) in H_2O solution. Analogous effects showing a smaller red shift (414 → 418 nm) and a very weak shoulder at ~439 nm for pH ~ 5 were observed in MeOH/H_2O solutions (Figure 2B). The hypochromism and red shift were interpreted [37–39] as a demonstration of the porphyrin ionic interaction with polypeptide matrices. Such an interpretation is strengthened by the negligible self-aggregation ability of TATP reported previously [48,54] and by the spectral pattern in the Soret region typical of monomeric porphyrin observed in the absence of PLGA (Figure 2). In the case of dioxan/H_2O solutions, the peak position (~418 nm) and the spectral band shape did not change significantly after the addition of PLGA and at different pH values, only slight hypochromism was observed at both pH (Figure 2C). This indicates that ionic interaction between cationic TATP and anionic PLGA takes place in aqueous and MeOH/H_2O solvents, while the dioxan/H_2O mixed solution substantially prevents the ionic interaction. Although the dioxan/H_2O solution at pH ~ 5 is an environment that supports very well the α-helix structure of the PLGA matrix, it is useless for the study of PLGA–TATP interactions. Most of the spectra in Figure 2 show negligible absorption which is typical of protonated TATP except for the spectrum of TATP–PLGA in MeOH/H_2O at pH ~ 5 (spectrum B, thick dashed line) where a shoulder at ~440 nm was observed. Therefore, most of the porphyrin molecules were present as free base in the conditions used. From the results presented in Figures 1 and 2 it follows that aqueous and MeOH/H_2O mixed solution represent an environment suitable for the study of interactions between PLGA and TATP.

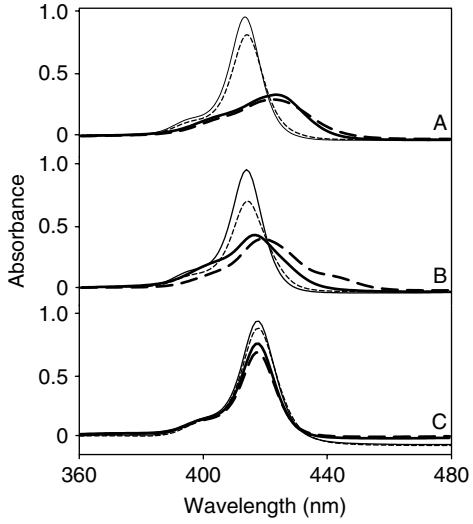

Figure 2 UV-VIS absorption of pure TATP (thin lines) and PLGA-TATP, $R = 100$ (thick lines) at pH ~ 8 (solid lines) and pH ~ 5 (dashed lines) in aqueous and mixed aqueous solution. (A) H_2O, (B) 40% MeOH/H_2O, (C) 50% dioxan/H_2O.

The Structure of the Polypeptide Part of Complexes

The structure of the polypeptide part of the complexes was investigated using VCD. First of all, it was found that the presence of TATP, $R = 100$, in D_2O and methanol-d_4/D_2O solutions prevented the precipitation of PLGA even at pH ~ 5, although pure PLGA precipitated from solutions under the same conditions. Therefore, unlike the pure PLGA, the PLGA–TATP complex in aqueous and mixed methanol-d_4/D_2O solutions

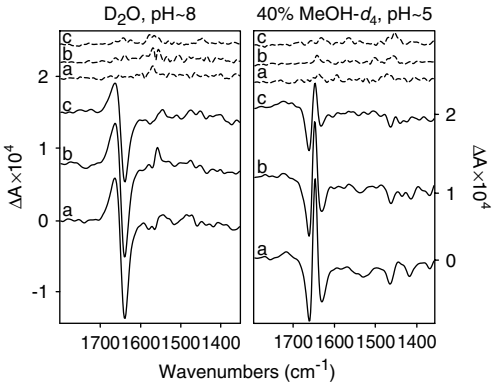

Figure 3 VCD spectra (solid lines) and noise spectra (dashed lines) of PLGA-TATP, $R = 100$, in D_2O at pH ~ 8 and in 40% methanol-d_4/D_2O at pH ~ 5, average molecular weight of PLGA MW = 50 300 (a), 17 000 (b), 10 900 (c).

was monitored using VCD for the whole studied interval of pH. Figure 3 shows the VCD spectra of PLGA–TATP in D_2O at pH ~ 8 and in 40% methanol-d_4/D_2O at pH ~ 5. The average molecular weight of the matrices varied from $M_W = 50\,300$ to 10 900 representing an average number of amino acid residues from 333 to 72. In D_2O at pH ~ 8, a negative couplet centred at 1653 cm^{-1} with negative and positive bands at 1639 and 1662 cm^{-1}, respectively, was observed for all polypeptides of the different chain lengths. VCD patterns were the same as for the case of pure PLGA solutions shown in Figure 1a–e. A reproducible decrease of the VCD signal accompanying the decrease of the polypeptide chain length was observed: the VCD intensities (expressed as peak-to-peak $\Delta A/A_{max}$ in amide I) for $PLGA_{17,000}$-TATP (Figure 3b) and $PLGA_{10,900}$-TATP (Figure 3c) reached, respectively, 92% and 70% of the intensity of $PLGA_{50,300}$-TATP (Figure 3a). This effect is in accordance with the molecular weight dependence of VCD intensity observed for poly-L-lysine having a PPII structure [14]. A similar dependence of the VCD spectra on the PLGA molecular weight was observed for PLGA–TATP in the methanol-d_4/D_2O solutions up to 40% of methanol-d_4 (spectra not shown).

In 40% methanol-d_4/D_2O at pH ~ 5, positive couplets with positive and negative peaks located at 1651 and 1663 cm^{-1}, respectively, were observed for polypeptides of all chain lengths. The VCD patterns obtained resemble a typical α-helix structure [14] apart from the intensity ratio of positive to negative peaks which was higher for the longest polypeptide chain than reported for other measurements of polypeptides in α-helix structure [12,17,21]. The decrease of the VCD intensity (peak-to-peak $\Delta A/A_{max}$ in amide I) accompanying the average molecular weight decrease was more pronounced than when the matrix possessed PPII structure: the VCD peak-to-peak $\Delta A/A_{max}$ in amide I for $PLGA_{17,000}$-TATP (Figure 3b) and $PLGA_{10,900}$-TATP (Figure 3c) reached, respectively, 70% and 50% of the $\Delta A/A_{max}$ corresponding to the longest matrix of $PLGA_{50,300}$-TATP (Figure 3a).

Interaction with porphyrins prevented the precipitation of PLGA at pH ~ 5 and at a concentration of about 0.4 mol/l. To obtain the α-helix structure in complexes demonstrated by a typical positive VCD couplet in amide I, the presence of methanol-d_4 was necessary. In an effort to test the stability and structure of complexes in aqueous solutions without methanol-d_4, another water soluble negatively charged porphyrin derivative TPPS was used which is known to produce porphyrin–porphyrin aggregates with positively charged porphyrins [41]. Figure 4 shows the VCD and absorption spectra of PLGA–TATP–TPPS, $R_{TATP} = R_{TPPS} = 100$ in D_2O at pH ~ 5 (spectrum (a)) where no precipitation was observed. The shape of the VCD spectrum differed significantly from the spectrum of PLGA–TATP obtained in mixed methanol-d_4/D_2O solution under the same pH (Figure 4c); instead of a positive couplet, a VCD pattern with two negative bands at 1632 and 1661 cm^{-1} of lower intensity, and a band at 1649 cm^{-1}, originally positive, were observed. In absorption spectra, asymmetric and symmetric COO^- characteristic bands at 1565 and 1408 cm^{-1}, respectively, as well as a shoulder at 1701 cm^{-1} corresponding to the carboxylic group were observed (Figure 4a, ABS). In the same Figure 4, the VCD and absorption spectra of PLGA–TATP in 40% methanol-d_4/D_2O at pH ~ 5 (Figure 4c) and pH ~ 8 (Figure 4d) are shown. The averages of these two VCD and absorption spectra give the patterns which are plotted as spectrum (b). The distinctive coincidence of the VCD as well as the absorption bands of experimental spectra (a) with calculated spectra (b) is evident. This fact is interpreted as a coexistence of both α-helix and PPII conformations in aqueous solution at pH ~ 5

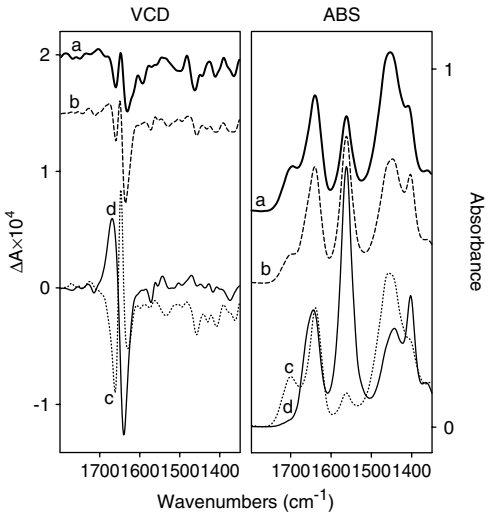

Figure 4 VCD and IR absorption spectra of PLGA-TATP-TPPS in D_2O at pH ~ 5, $R_{TATP} = R_{TPPS} = 100$ (a), simulated spectra (b). VCD and IR spectra of PLGA-TATP in the 40% methanol-d_4/D_2O, $R_{TATP} = 100$ at pH ~ 5 (c) and pH ~ 8 (d).

when both the porphyrins TATP and TPPS are present. Although a mixture of PII and α-helical structural segments might not be manifested as a linear superposition of spectral patterns typical of each structure, this observation can be considered as a qualitative indication of the simultaneous presence of both structural segments because of the characteristic sensitivity of VCD to the structural features which is demonstrated by the sign, shape and positions of the VCD signals.

Figure 5 shows the VCD spectra of PLGA–TATP in the D_2O solutions at pH $\sim$ 5 for different values of the ratio R. The observed VCD patterns differ from those typical for the α-helix or PPII structures. The observed spectral shape was compared with a simulated VCD spectrum obtained as the weighted average of VCD spectra of PLGA–TATP in 40% methanol-d_4/D_2O at pH $\sim$ 5, the typical α-helix shape, and at pH $\sim$ 8, the typical PPII shape, shown in Figure 4c,d. For $R = 100$, a significant intensity decrease of the whole VCD pattern and a slight red shift of the maximum were observed. The negative band at 1632 cm^{-1} remained strong and a new positive band at 1679 cm^{-1} was observed (Figure 5a). The spectral pattern observed was simulated by a weighted average of VCD spectra typical for PPII and α-helix structures in the ratio of 2 : 1. The increased TATP concentration in the solution caused progressive changes in VCD. The VCD patterns obtained for PLGA-TATP, $R = 38$ and 20 (Figure 5b, c), were simulated by the weighted average of typical PPII and α-helix spectra in the ratios 3 : 1 and 4 : 1, respectively. The contribution of the band at 1649 cm^{-1}, originally positive, typical for the α-helix conformation decreased, the negative band at 1661 cm^{-1} totally disappeared, and the weak positive band at 1679 cm^{-1} was enhanced and shifted to 1671 cm^{-1}. Although the VCD magnitude in the simulated spectra was higher than in the experimental ones, quite good coincidence between spectral shapes was observed.

ECD Spectra of PLGA–TATP Complexes

The ECD spectra of the porphyrin part of PLGA–TATP complexes in the Soret region are shown in Figure 6. While the addition of PLGA into the aqueous solution of TATP induced a negligible ECD signal of TATP at pH $\sim$ 8, in the presence of 40% MeOH/H_2O, a slight ECD pattern was observed (Figure 6a). However, at pH $\sim$ 5 in both aqueous and MeOH/H_2O solutions, a very strong couplet was observed (Figure 6b). In the aqueous solution, the couplet was centred at 421 nm and the positive and negative bands were located at 428 and 415 nm, respectively; in the presence of methanol, the ECD pattern was enhanced almost three times compared with the aqueous solution. The centre of the couplet was shifted to 419 nm and the strong positive and negative bands occurred at 428 and 414 nm, respectively. Besides this characteristic positive couplet centred at the absorption maximum, a pair of two distinctive sidebands, the negative and positive at 444 and 395 nm, respectively, was observed. Analogous sidebands were obtained by calculation [46] of ECD spectra and will be discussed later.

The ECD spectra of PLGA–TATP were also measured in the region suitable for peptide study (190–260 nm) as a proof of the matrix conformation at the concentrations used in ECD measurement (Figure 6). At pH $\sim$ 8, a negative band at 198 nm was observed for both MeOH/H_2O and H_2O solutions (spectra (a)). This shape of ECD spectra is characteristic for the PPII conformation [9,56]. At pH $\sim$ 5, two negative bands were observed at 222 and 209 nm in both MeOH/H_2O as well as aqueous solutions (spectra (b)). Such an ECD pattern is characteristic for the α-helix conformation [9,56]. The intensity of ECD was influenced by the solvent: the ECD intensity was observed to be higher

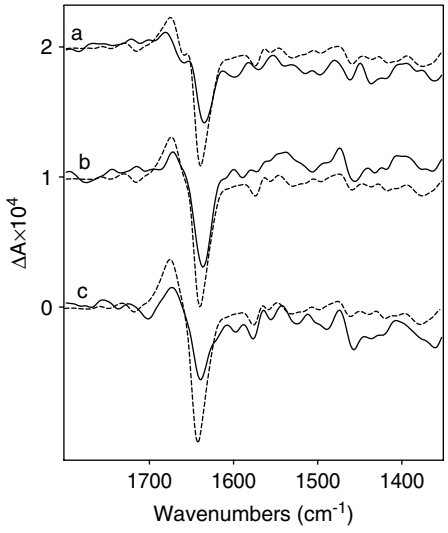

Figure 5 Experimental (solid lines) and simulated (dashed lines) VCD spectra of PLGA-TATP in D_2O, pH $\sim$ 5, $R_{TATP} = 100$ (a), 38 (b), 20 (c).

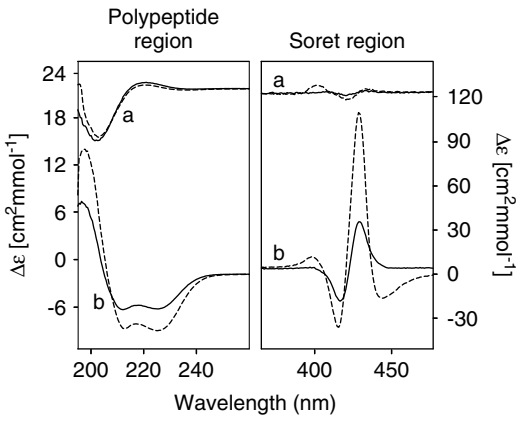

Figure 6 ECD spectra of PLGA-TATP, $R = 100$, in H_2O (solid lines) and in 40% MeOH/H_2O (dashed lines) in the polypeptide and the Soret regions, pH $\sim$ 8 (a), pH $\sim$ 5 (b).

in MeOH/H_2O solution than in pure H_2O, which coincides with the α-helix supporting properties of alcohols. The changes of ECD spectra between PLGA-TATP in pure aqueous and MeOH/H_2O solutions were not as distinctive for PPII as for the α-helix conformations (cf. spectra (a) and (b)). The behaviour of PLGA in the solution was strongly dependent on the polypeptide concentration. While the samples at pH $\sim$ 5 precipitated at a concentration of $\sim$0.4 mol/l suitable for VCD and IR absorption measurements, such effects were not observed in concentrations of 0.001–0.01 mol/l used for ECD and UV-VIS absorption.

DISCUSSION

The Secondary Structure of PLGA

The synthetic homopolypeptides serve as model substances for the study of proteins. This paper focused on PLGA as a typical polymer, whose secondary structure is strongly influenced by the physicochemical properties of the solution, mainly by the pH value. In spite of the fact that this macromolecule has been studied for more than 50 years, there are still some points of interest that have not been described thoroughly.

The forces affecting the secondary structure of PLGA are generally coulombic interactions, more specifically hydrogen bonds. This kind of interaction strongly depends on pH. In addition, the pH values influence the dissociation of the PLGA side chain groups and therefore their dissociation constant (pK = 4.6) [30] plays a key role. At pH $\sim$ 8, PLGA adopts a conformation that is characterized as a short left-handed helical chain composed of polyproline II like 3_1-helices [50]. It was shown recently [57] that the homotripeptide L-glutamyl-L-glutamyl-L-glutamate adopts an extended polyproline II helix conformation which confirms the short range of this structure. At pH $\sim$ 8, most of the carboxylic groups in the side chains exist as carboxylates which are solvated in aqueous solutions and therefore precipitation is avoided even in the high concentrations used in IR spectroscopy.

The relative permittivity is another factor that influences the secondary structure of polypeptides. The 20% and 40% presence of methanol-d_4 in the mixed methanol-d_4/D_2O solvents caused negligible changes of the VCD pattern. However, 60% methanol-d_4 and 50% dioxan-d_8 in D_2O substantially reduced the intensity of the VCD pattern compared with that in aqueous solution (Figure 1). The relative permittivity ε_r of pure methanol ($\varepsilon_r = 32$) and dioxan ($\varepsilon_r = 2.2$) was markedly lower than the ε_r of pure water (ε_r = 80). The stabilizing effect of the solvent on the PPII structure is caused by strong hydrogen (deuterium) bonding between polypeptide and the $H_2O(D_2O)$ solvent molecules. Hydrogen bonding is an interaction that depends significantly on the relative permittivity of the solvent. Due to this fact, the stabilizing effect of a solvent with a low value of ε_r on the PPII structure is decreased and therefore a decrease in the VCD intensity typical of PPII is observed. Such phenomena should be a consequence of the partial transition of a polyproline II like secondary structure to a secondary unordered polypeptide chain. These observations support the concept [14] that the PPII conformation is a locally oriented structure which is stabilized by appropriate solvents. The importance of the solvent for the stabilization of the PPII structure was revealed recently by a molecular dynamic approach that indicated a groove around the peptide backbone that is strongly hydrated [58].

Under strong acidic pH the system adopts the α-helix. In this case, the predominant part of the PLGA side chain carboxylic groups exist in non-ionized form; at pH $\sim$ 5 only about 30% of the carboxylic groups remain as carboxylates, hence the solvation of PLGA in D_2O ($\varepsilon_r = 80$) is suppressed. Although it is almost generally accepted that at pH $\sim$ 5 PLGA adopts an α-helix structure, in a concentration suitable for vibrational spectroscopy, $\sim$0.1 mol/l, PLGA irreversibly precipitates and therefore it is not possible to perform optical spectral measurements. The addition of dioxan-d_8 (solvent with low $\varepsilon_r = 2.2$) prevents the undesirable precipitation; the PLGA α-helix structure was obtained in dioxan-d_8/D_2O = 1/1 (v/v) solvent. Simultaneously, such a mixed solvent prevents ionic interaction with porphyrins.

The Interaction of PLGA with TATP

Using UV-VIS absorption it was shown that the interaction between PLGA and cationic TATP occurs in aqueous and mixed MeOH/H_2O solutions (Figure 2). TATP was chosen as a cationic porphyrin derivative appropriate for ionic interactions as it possesses sufficient solubility in polar solvents with the required stability in a wide pH region (5–12). Another very important property of TATP is a very low tendency for self-aggregation in solution, especially as the monomeric form of porphyrin is generally more suitable for the study of specific polypeptide/porphyrin interaction compared with poorly spatially characterized porphyrin aggregates. The monomeric form of TATP was proved by the absorption band at 414 nm. In the presence of a polypeptide matrix, the characteristic spectral red shift and the hypochromic effect were observed in aqueous and 40% MeOH/H_2O solutions. These spectral changes are typical of polypeptide–porphyrin interactions [37–39]; however, it could be a consequence of porphyrin–porphyrin self-aggregation of the J-type or porphyrin–porphyrin interaction mediated by their binding to the matrix. The TATP rate constant of J-aggregate formations is the smallest of the different

meso-phenyl substituents [48], however, the rate of formation increases with special treatment, for example by vigorous stirring and increased ionic strength [48]. Because the red shift and hypochromism were not observed in TATP solutions without PLGA at the same concentration of TATP, we believe that the polypeptide–porphyrin complexation or porphyrin–porphyrin interaction mediated by their binding to PLGA are the preferred interactions occurring in the systems studied.

The complexation of PLGA with porphyrins influences both the components and *vice versa.* The secondary structure of the polypeptide part of PLGA–TATP was determined by VCD, which has proved its high sensitivity to the spatial structure of macromolecules, and ECD, which was used to confirm the secondary structure of PLGA at small concentrations. The ECD spectroscopy was also used to study the porphyrin part of the complexes.

The precipitation of PLGA at strong acidic pH may be caused by non-covalent interactions of the COOH side chain groups. Due to the ionic interactions with PLGA the TATP molecules work as molecular spacers that are spread along the whole polypeptide chain and prohibit precipitation. However, due to the appropriate spatial arrangement of the porphyrin molecules interacting with PLGA [40], π-π interactions between porphyrin rings occur, influencing the matrix conformation and *vice versa*. It was found that the intensity of the positive couplet in amide I region characteristic of the α-helix structure of PLGA–TATP depends on the polypeptide chain length. A similar dependence was less significant for the PPII structure than for the α-helix conformation of PLGA (Figure 3). This difference is explained by the fact that the α-helix structure is stabilized by hydrogen bridges in the peptide bonds, while the PPII structure is also supported by the solvation of the carboxylate side chain groups in polar solvents.

When pH decreases (pH $\sim$ 5) the structure of PLGA-TATP in 40% methanol-d_4/D_2O turns from PPII to α-helix. The presence of TATP and a decrease in relative permittivity of the solvent by the addition of methanol serve as α-helix supporting conditions. To separate the influence of methanol, PLGA-TATP-TPPS at pH $\sim$ 5 in pure D_2O was studied. The system provided a clear solution even at pH $\sim$ 4. However, the VCD patterns in amide I region did not correspond to any well known structures, e.g. α-helix or PPII (Figure 4). The shape of the observed VCD pattern can be obtained as the weighted average of VCD patterns typical for α-helix and PPII like structures. The contribution of the VCD pattern characteristic for the α-helix structure is evident from the positive band at 1649 cm^{-1} and the negative band at 1661 cm^{-1}. The intensity of both bands is reduced by overlapping the negative VCD couplet, which is typical for PPII. Simultaneously, this couplet contributes to the observed spectrum by a second negative VCD band at 1632 cm^{-1}. It follows from the coincidence between the simulated and the experimental spectra that PLGA can adopt both α-helix and PPII conformations under the specific conditions at the same time. Although the band position and shape of the simulated and experimental VCD spectra are very similar, the intensities differ. This fact is explained by the existence of spatially unordered polypeptide chains in solution, which are inactive in the VCD spectra. This effect probably occurs only close to the state of equilibrium between the two conformations.

The effect of ionic interaction in the PLGA-TATP complex in D_2O at pH $\sim$ 5 was studied further by observation of the influence of different PLGA/TATP ratios on the VCD spectra of the polypeptide part of the complexes (Figure 5). A decrease of the ratio R progressively favours the content of PPII structure. However, without the presence of TPPS the content of α-helix was never equal to PPII according to the simulation of spectra presented in Figure 5. It means that the presence of TATP prevents sample precipitation and supports the formation of α-helix in D_2O in the presence of alcohol or TPPS.

The ECD spectra in the Soret region prove that the interaction of TATP with PLGA induces the optical activity of TATP, which strongly depends on the matrix conformation. In the presence of the PPII structure of PLGA, no distinctive ECD spectral changes were observed. However, if PLGA adopted the α-helix conformation, enhanced ECD intensity was observed: a three times higher intensity occurred in the MeOH/H_2O solution compared with pure aqueous solution, which correlates with the different α-helix content proved by the typical VCD and ECD signals in the amide I and the peptide regions, respectively (Figure 3, Figure 6).

Besides the characteristic couplet in the Soret region, which occurs due to porphyrin bonding to the PLGA α-helix, two distinctive sidebands occur in MeOH/H_2O solution at pH $\sim$ 5 (Figure 6b). These sidebands were discussed in a detailed study by Pescitelli [46] *et al.*, in which the effect of mutual orientation of porphyrins on ECD spectra was thoroughly tested experimentally and theoretically. The existence of the very distinctive sidebands was explained [46] as a consequence of a very strong coupling between some components of the coupled circular oscillators underlying the face-to-face π-π stacking. A comparison of our experimental ECD spectra with the published calculated spectra leads to the conclusion that the TATP molecules in the PLGA-TATP complex in α-helix structure are bonded to the matrix parallel to each other at a very short distance, enabling strong porphyrin coupling due to π-π stacking between the porphyrin rings. Such an interaction strongly contributes also to the intensity of the dominant couplet and explains the observed increase in the

magnitude of the observed ECD signal. Moreover, the 'secondary' interactions between porphyrins bound in an appropriate manner to the α-helical matrix provide a stabilizing effect on the α-helix conformation of the complexes. On the other hand, porphyrins bound to the PLGA matrix possessing the PPII structure are not in positions that favour the π-π stacking.

CONCLUSION

This VCD and ECD study focused on the study of interactions of poly-L-glutamic acid and *meso*-tetrakis(α-trimethylammonio-*p*-tolyl)porphyrin tetrabromide and the variations of spatial structure of both interacting agents. Appropriate mixed solutions and pH values were found suitable for the study of the PLGA-TATP complexes for both the main conformations of PLGA – PPII and α-helix structures. It was shown that not only the porphyrin part of the complexes is influenced by the conformation of the polypeptide matrix but the porphyrin affects the polypeptide part as well. The interaction of PLGA with TATP prevents the precipitation at pH $\sim$ 5 which occurs for pure PLGA at concentrations higher than 0.1 mol/l. The VCD pattern typical for both the α-helix and PPII structures depends on the length of the polypeptide chain: the longer chain possessed a higher VCD signal for the both polypeptide conformations. It was shown that the interaction of porphyrin with PLGA leads to the simultaneous existence of both the α-helix and PPII structure in pure aqueous solution at acidic pH without precipitation. The ratio of both the conformations was influenced by the ratio of porphyrin/amino acid residue: a higher relative content of porphyrin caused a higher content of the PPII conformation of PLGA.

The ECD results show that the induction of the porphyrin optical activity depends on the matrix configuration. The highest ECD signal was observed in the case of a high content of α-helix in the matrix structure which occurs in MeOH/H_2O solutions at pH $\sim$ 5. The presence of the α-helix polypeptide matrix is the driving force for the formation of porphyrin assemblies which significantly adopt the spatial coordination of the polypeptide template. Hence, the originally achiral porphyrins create objects with specific geometry providing optical activity. Besides the main ECD pattern in the Soret region, the porphyrin assemblies provide significant ECD sidebands on both the long and short edges of the main porphyrin signal predicted previously by the study of the bis-porphyrins possessing the π-π interaction. This coincidence leads to the conclusion that the assembled porphyrins are bonded to the matrix in methanol/H_2O solutions at pH $\sim$ 5 in a way enabling close mutual porphyrin face-to-face interaction.

Acknowledgements

We are grateful to Professor Vladimír Král for providing us with the porphyrin samples and for stimulating discussions. This work was supported by grants MSM 6046137307 from the Ministry of Education, Youth and Sports of the Czech Republic, 203/02/0328 from Grant Agency of the Czech Republic, and IAA 4055104 from Grant Agency of Academy of Sciences of the Czech Republic.

REFERENCES

1. Sternberg ED, Dolphin D, Bruckner C. Porphyrin-based photosensitizers for use in photodynamic therapy. *Tetrahedron* 1998; **54**: 4151–4202.
2. Stryer L. Introduction to protein structure and function. In *Biochemistry*, WH Freeman: San Francisco, 1981; 11–42.
3. Jackson M, Haris PI, Chapman D. Fourier transform infrared spectroscopic studies of lipids, polypeptides and proteins. *J. Mol. Struct.* 1989; **214**: 329–355.
4. Keiderling TA, Silva RAGD. Conformational studies using infrared techniques. In *Houben-Weyl Methods of Organic Chemistry*, Vol. E22a Synthesis of Peptides and Peptidomimetics, Goodman M (ed.). Thieme Medical Publishers: New York, 2004; 715–738.
5. Kishi S, Santos J, Ishii O, Ishikawa K, Kunieda S, Kimura H, Shoji A. Synthesis and conformational study of silk model polypeptides $[Ala\text{-}Gly]_{12}$ by solid-state NMR. *J. Mol. Struct.* 2003; **649**: 155–167.
6. Murata K, Kono H, Katoh E, Kuroki S, Ando I. A study of conformational stability of polypeptide blends by solid state two-dimensional ^{13}C-^{1}H heteronuclear correlation NMR spectroscopy. *Polymer* 2003; **44**: 4021–4027.
7. Pascal SM, Cross TA. Polypeptide conformational space: dynamics by solution NMR disorder by x-ray crystallography. *J. Mol. Biol.* 1994; **241**: 431–439.
8. Doty J. Polypeptides. VI. Poly-α-L-glutamic acid: preparation and helix – coil conversion. *J. Am. Chem. Soc.* 1956; **78**: 497–498.
9. Sreerama N, Woody RW. Circular dichroism of peptides and proteins. In *Circular Dichroism: Principles and Applications*, Berova N, Nakanishi K (eds). John Wiley & Sons, Inc.: New York, 2000; 601–620.
10. Barron LD, Hecht L. Vibrational Raman optical activity: from fundamentals to biochemical applications. In *Circular Dichroism: Principles and Applications*, Berova N, Nakanishi K (eds).: John Wiley: New York, 2000; 667–701.
11. Dukor RK, Nafie LA. Vibrational optical activity of pharmaceuticals and biomolecules. In *Encyclopedia of Analytical Chemistry*, Mayers RA (ed.). John Wiley & Sons Ltd: Chichester, 2000; 1–15.
12. Freedman TB, Nafie LA, Keiderling TA. Vibrational optical activity of oligopeptides. *Biopolymers* 1995; **37**: 265–279.
13. Nafie LA. Vibrational optical activity. *Appl. Spectrosc.* 1996; **50**: 14A–26A.
14. Keiderling TA, Silva RAGD, Gorm Y, Dukor RK. Vibrational circular dichroism spectroscopy of selected oligopeptide conformations. *Bioorg. Med. Chem.* 1999; **7**: 133–141.
15. Lal BB, Nafie LA. Vibrational circular dichroism in amino acids and peptides. 7. Amide stretching vibrations in polypeptides. *Biopolymers* 1982; **21**: 2161–2183.
16. Polavarapu PL, Zhao Ch. Vibrational circular dichroism: a new spectroscopic tool for biomolecular structural determination. *Fresenius J. Anal. Chem.* 2000; **366**: 727–734.
17. Sen AC, Keiderling TA. Vibrational circular dichroism of polypeptides. III. Film studies of several α-helical and β-sheet polypeptides. *Biopolymers* 1984; **23**: 1533–1545.

18. Sen AC, Keiderling TA. Vibrational circular dichroism of polypeptides. II. Solution amide II and deuteration results. *Biopolymers* 1984; **23**: 1519–1532.
19. Yasui SC, Keiderling TA. Vibrational circular dichroism of polypeptides. 8. Poly(lysine) conformations as a function of pH in aqueous solution. *J. Am. Chem. Soc.* 1985; **108**: 5576–5581.
20. Keiderling TA. Peptide and protein conformational studies with vibrational circular dichroism and related spectroscopies. In *Circular Dichroism: Principles and Applications*, Berova N, Nakanishi K (eds). John Wiley: New York, 2000; 621–666.
21. Silva RAGD, Yasui SC, Kubelka J, Formaggio F, Crisma M, Toniolo C, Keiderling TA. Discriminating 3_{10} from α-helices: vibrational and electronic CD, and IR absorption study of related aib-containing oligopeptides. *Biopolymers* 2002; **65**: 229–243.
22. Cheeseman JR, Frisch MJ, Devlin FJ, Stephens PJ. Ab initio calculation of atomic axial tensors and vibrational rotational strengths using density functional theory. *Chem. Phys. Lett.* 1996; **252**: 211–220.
23. Gulotta M, Goss DJ, Diem M. IR vibrational CD in model deoxyoligonucleotides: Observation of the B – Z phase transition and extended coupled oscillator intensity calculations. *Biopolymers* 1989; **28**: 2047–2058.
24. Stephens PJ, Chabalowski CF, Devlin FJ, Jalkanen KJ. Ab initio calculation of vibrational circular dichroism spectra using large basis set MP2 force fields. *Chem. Phys. Lett.* 1994; **225**: 247–257.
25. Stephens PJ, Devlin FJ, Cheeseman JR, Frisch MJ, Mennucci B, Tomasi J. Prediction of optical rotation using density functional theory: 6,8-dioxabicyclo[3.2.1]octanes. *Tetrahedron: Asymmetry* 2000; **11**: 2443–2448.
26. Bouř P, Keiderling TA. Ab initio simulations of the vibrational circular dichroism of coupled peptides. *J. Am. Chem. Soc.* 1993; **115**: 9602–9607.
27. Bouř P, Sopková J, Bednářová L, Keiderling TA. Transfer of molecular property tensors in cartesian coordinates: A new algorithm for simulation of vibrational spectra. *J. Comput. Chem.* 1997; **18**: 646–659.
28. Bouř P, Kubelka J, Keiderling TA. Simulations of oligopeptide vibrational CD: Effects of isotopic labeling. *Biopolymers* 2000; **53**: 380–395.
29. Bouř P, Kubelka J, Keiderling TA. Ab initio quantum mechanical models of peptide helices and their vibrational spectra. *Biopolymers* 2002; **65**: 45–59.
30. Olander DS, Holtzer A. The stability of the polyglutamic acid α helix. *J. Am. Chem. Soc.* 1968; **90**: 4549–4560.
31. Gangs PJ, Lyu PC, Manning MC, Woody RW, Kallenbach NR. The helix-coil transition in heterogenous peptides with specific side-chain interactions: theory and comparison with spectral data. *Biopolymers* 1991; **31**: 1605–1614.
32. Krittanai C, Johnson J. Correcting the circular dichroism spectra of peptides for contributions of absorbing side chains. *Anal. Biochem.* 1997; **253**: 57–64.
33. Nagasawa M, Holtzer A. The helix-coil transition in solutions of polyglutamic acid. *J. Am. Chem. Soc.* 1963; **86**: 538–543.
34. Paoletti S. Conformational transition of poly(α-L-glutamic acid). A polyelectrolytic approach. *Biophys. Chem.* 1989; **34**: 301–309.
35. Geier III GR, Sasaki T. The design, synthesis and characterization of a porphyrin-peptide conjugate. *Tetrahedron Lett.* 1997; **38**: 3821–3824.
36. Huffman DL, Suslick KS. Hydrophobic interactions in metalloporphyrin-peptide complexes. *Inorg. Chem.* 2000; **39**: 5418–5419.
37. Ikeda S, Nezu T, Gotthold E. Induced CD and interaction of some porphyrin derivatives with α-helical polypeptides in aqueous solutions. *Biopolymers* 1991; **31**: 1257–1263.
38. Nezu T, Ikeda S. Induction of circular dichroism of symmetrical porphyrins bound to random coil polypeptides in aqueous solutions. *Int. J. Biol. Macromol.* 1993; **15**: 101–103.
39. Nezu T, Ikeda S. Induced circular dichroism of a cationic porphyrin bound to α-helical poly(L-glutamic acid) and β-form poly(S-carboxymethyl-L-cysteine) in aqueous solutions. *Bull. Chem. Soc. Jpn* 1993; **66**: 18–24.
40. Purrello R, Scolaro LM, Bellacchio E, Gurrieri S, Romeo A. Chiral H- and J-type aggregates of *meso*-tetrakis(4-sulfonatophenyl)porphine on helical polyglutamic acid induced by cationic porphyrins. *Inorg. Chem.* 1998; **37**: 3647–3648.
41. Lauceri R, Raudino A, Scolaro LM, Micali N, Purrello R. From achiral porphyrins to template-imprinted chiral aggregates and further. Self-replication of chiral memory from scratch. *J. Am. Chem. Soc.* 2002; **124**: 894–895.
42. Berova N, Nakanishi K. Exciton chirality method: Principles and applications: In *Circular Dichroism: Principles and Applications*, Berova N, Nakanishi K (eds). John Wiley: New York, 2000; 337–382.
43. Borovkov VV, Lintuluoto JM, Inoue Y. Supramolecular chirogenesis in zinc porphyrins: Mechanism, role of guest structure, and application for the absolute configuration determination. *J. Am. Chem. Soc.* 2001; **123**: 2979–2989.
44. Borovkov VV, Lintuluoto JM, Sugeta H, Fujiki M, Arakawa R, Inoue YJ. Supramolecular chirogenesis in zinc porphyrins: equilibria, binding properties, and thermodynamics. *J. Am. Chem. Soc.* 2002; **124**: 2993–3006.
45. Borovkov VV, Hembury GA, Inoue Y. The origin of solvent-controlled supramolecular chirality switching in a bis(zinc-porphin) system. *Angew. Chem. Int. Ed. Engl.* 2003; **42**: 5310–5314.
46. Pescitelli G, Gabriel S, Wang Y, Fleischhauer J, Woody RW, Berova N. Theoretical analysis of the porphyrin-porphyrin exciton interaction in circular dichroism spectra of dimeric tetraarylporphyrins. *J. Am. Chem. Soc.* 2003; **125**: 7613–7628.
47. Urbanová M, Setnička V, Král V, Volka K. Noncovalent interactions of peptides with porphyrins in aqueous solutions. *Biopolymers* 2001; **60**: 307–316.
48. Kubát P, Lang K, Anzenbacher P Jr, Jursíková K, Král V, Ehrenberg B. Interaction of novel cationic meso-tetraphenylporphyrins in the ground and excited states with DNA and nucleotides. *J. Chem. Soc. Perkin Trans. 1* 2000; 933–941.
49. Aoudia M, Rodgers MAJ. Photoprocess in self-assembled complexes of oligopeptides with metalloporphyrins. *J. Am. Chem. Soc.* 1997; **119**: 9063–9064.
50. Dukor RK, Keiderling TA. Reassessment of the random coil conformation: Vibrational CD study of proline oligopeptides and related polypeptides. *Biopolymers* 1991; **31**: 1747–1761.
51. McColl IH, Blanch EW, Lutz H, Kallenbach NR, Barron LD. Vibrational Raman optical activity characterization of poly(L-proline) II helix in alanine oligopeptides. *J. Am. Chem. Soc.* 2004; **126**: 5076–5077.
52. Makovec T. Poly-L-glutamic acid and poly-L-lysine: model substances for studying secondary structures of proteins. *Biochem. Mol. Biol. Educ.* 2000; **28**: 244–247.
53. Arunkumar AI, Kumar TKS, Yu C. Non-specific helix induction in charged homopolypeptides by alcohols. *Biochim. Biophys. Acta* 1997; **1338**: 69–76.
54. Kubát P, Lang K, Procházková K, Anzenbacher P Jr. Self-aggregates of cationic *meso*-tetratolylporphyrins in aqueous solutions. *Langmuir* 2003; **19**: 422–428.
55. Urbanová M, Setnička V, Volka K. Measurements of concentration dependence and enantiomeric purity of terpene solutions as a test of a new commercial VCD spectrometer. *Chirality* 2000; **12**: 199–203.
56. Greenfield N, Fasman GD. Computed circular dichroism spectra for the evaluation of protein conformation. *Biochemistry* 1969; **8**: 4108–4116.
57. Eker F, Griebenow K, Cao X, Nafie LA, Schweitzer-Stenner R. Tripeptides with ionizable side adopt a perturbed polyproline II structure in water. *Biochemistry* 2004; **43**: 613–621.
58. Garcia AE. Characterization of non-alpha helical conformations in Ala peptides. *Polymer* 2004; **45**: 669–676.